

**Military Technical College
Kobry El-Kobbah,
Cairo, Egypt**



**11th International Conference
on Electrical Engineering
ICEENG 2018**

Encoding, Decoding and Sidelobes Cancellation of Nested Compound Binary phase coded signal

A. Ahmed Sobhy*, B. Abd El-Rahman H. Elbardawiny*, C. Fathy M. Ahmed*, and Mamdouh Hassan*

ABSTRACT

One of the methods for improving maximum radar range performance is increasing the average transmitted power. In this paper, this objective is achieved by nesting binary phase coded waveforms with different lengths. The decoding of these nested codes leads to appearance of high sidelobes which are canceled by nesting corresponding optimum filters. The hardware structure of the encoder and sidelobes cancellation processor of these nested codes are simply realized by cascading the corresponding original Barker code filters with changing the filter length in each cascaded level.

KEY WORDS

Phase Coded Signal, Compound Barker Codes, Pulse Compression, Sidelobe Reduction

1. Introduction

Pulse compression coding is used in radar applications to get the benefits of high average power of a long pulse along with the range resolution of a short pulse. Binary phase coded signal is one of the most famous techniques in pulse compression where The binary code consists of a sequence of In-phase (+1 or (0°)) and out of phase (-1 or (180°)) relating to a reference signal [1]. Barker codes are known as the smallest achieved peak sidelobe level (PSL) equal to 1 [2] However, the longest available Barker code is of length 13. For longer phase coded signals beyond 13, an exhaustive search

* Egyptian Armed Forces.

for minimum peak sidelobe level (PSL) sequences are presented in [3,4] up to length (N=105). Figure (1) shows the Peak sidelobe level of the best known binary code sequences. Figure (2) shows that we can obtain peak to side lobe ratio (PSLR) results better than those of Barker codes although the PSL is greater than 1.

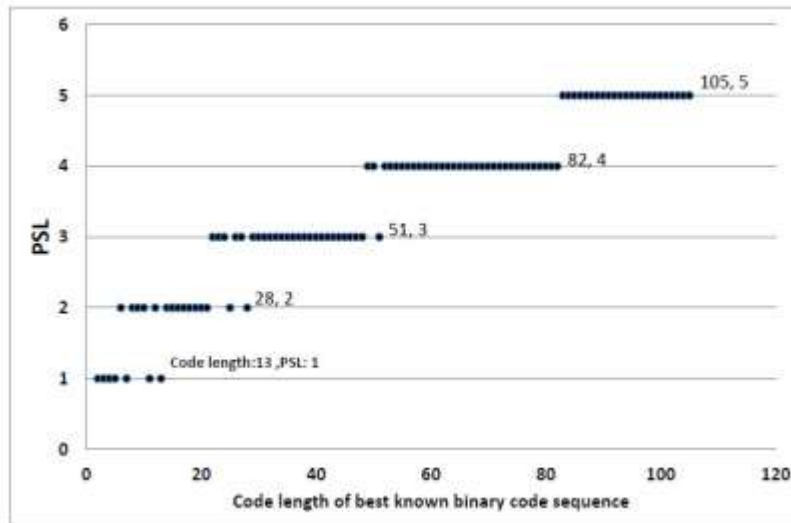


Fig.1. PSL of best known Binary code sequences

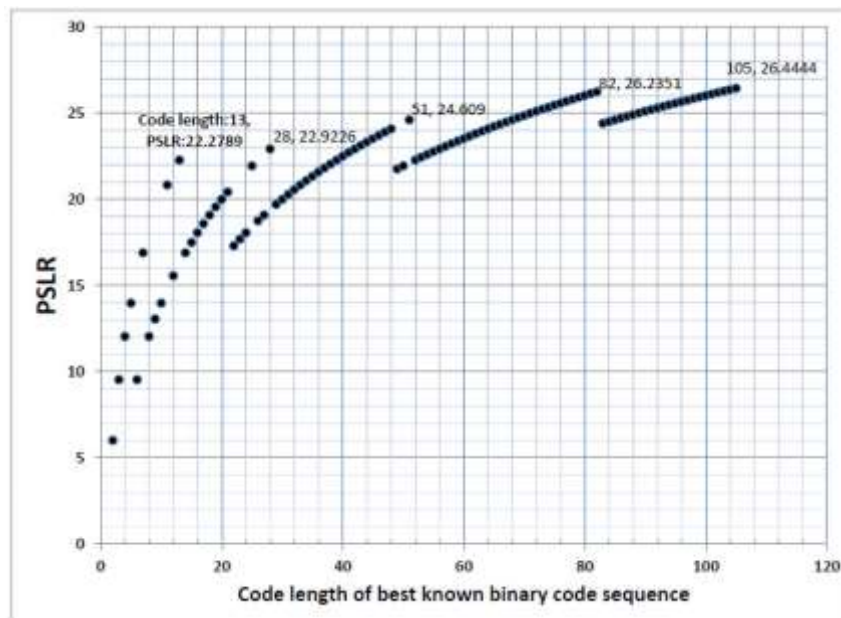


Fig.2. PSLR of best known Binary code sequences

Another method for generating longer codes is to compound exciting codes [5]. For compound codes, a child Barker code with length N_1 is repeated a number of times equal to the number of elements in a parent Barker code N_2 . Each repetition of the child code is reversed in phase or not depending on the value of each element in the parent code. The resulted code length is calculated as:

$$N_{1,2} = N_1 \times N_2 \tag{1}$$

The resulted code can be repeated as child of another Barker code with length N_3 which can be considered in this case as the grandfather code. Consequently, the code length of the resulted code is increased N_3 times. This methodology in generating nested compound codes has no end or limit in the code length. The resulted code length of the nested compound codes depends on the number of parent level L and the code length of each level. The length of the nested compound code is calculated as:

$$N = \prod_{i=1}^L N_i \tag{2}$$

The nested compound codes are long enough to enhance the signal to noise ratio S/N but the sidelobe level will remain high. These long codes will not enhance the PSLR without side lobe suppression. In this paper, an extended version of optimum filter which innovated by authors [6] is presented to totally remove sidelobes of nested compound codes.

2. Encoder and Decoder of Nested Compound Codes

2.1 Encoder of nested compound codes

To find a general formula for generating a compound codes, let us consider a simple case of combining Barker code B_3 of length equal 3 as a child code of parent code B_5 . The child code B_3 is represented as:

$$B_3 = \{+1, +1, -1\} \tag{3}$$

Its encoder has a transfer function which denoted as $H_3(Z)$.

The parent code B_5 is represented as:

$$B_5 = \{+1, +1, +1, -1, +1\} \tag{4}$$

Its encoder is denoted as $H_5(Z)$.

By repeating the child code B_3 five times (the length of the parent code $N_2 = 5$) and changing the phase depending on the parent code elements. The compound code becomes on the form:

$$\begin{aligned}
 B_{3,5} = & \{ \{ +1, +1, -1 \}, \\
 & \{ +1, +1, -1 \}, \\
 & \{ +1, +1, -1 \}, \\
 & \{ -1, -1, +1 \}, \\
 & \{ +1, +1, -1 \} \}
 \end{aligned} \tag{5}$$

The transfer function of the encoder of this code is:

$$\begin{aligned}
 H(Z) = & 1 + Z^{-1} - Z^{-2} + Z^{-3} + Z^{-4} - Z^{-5} \\
 & + Z^{-6} + Z^{-7} - Z^{-8} - Z^{-9} - Z^{-10} \\
 & + Z^{-11} + Z^{-12} + Z^{-13} - Z^{-14}
 \end{aligned} \tag{6}$$

Simplifying equation (6), the transfer function becomes:

$$H(Z) = (1 + Z^{-1} + Z^{-2})(1 + Z^{-3} + Z^{-6} - Z^{-9} + Z^{-12}) \tag{7}$$

$$= H_3(Z)H_5(Z^3) \tag{8}$$

From equation (1), the resulted code length is 15.

For generalization, if a code B_{N_1} of length N_1 is compound as a child code with another parent code B_{N_2} of length N_2 the encoder transfer function can be written as:

$$H(Z) = H_{N_1}(Z) \times H_{N_2}(Z^{N_1}) \tag{9}$$

For nested compound codes, the generated code in (9) becomes a child of another code B_{N_3} . Thus, the encoder for nested compound codes becomes on the form:

$$H(Z) = H_{N_1}(Z) \times H_{N_2}(Z^{N_1}) \times H_{N_3}(Z^{N_1 N_2}) \tag{10}$$

The general formula of the transfer function for the Encoder of L level nested compound codes is written as:

$$H(Z) = \prod_{i=1}^L H_{N_i}(Z^{\prod_{k=1}^{i-1} N_k}) \tag{11}$$

2.2 Decoder of nested compound codes

Let the transfer function of matched filter for Barker code with length N is denoted by $H_{RN}(Z)$. Using the same methodology that has been used to find the encoder transfer function of nested compound codes, the general formula of the matched can be written as:

$$H_R(Z) = \prod_{i=1}^L H_{RN_i}(Z^{\prod_{k=1}^{i-1} N_k}) \tag{12}$$

Equation (12) represents the processing for the code of length $(N_1 \times N_2 \dots \times N_L)$. The autocorrelation function ACF of the code $B_{3,5}$ is found to be:

$$r(n) = [-1, 0, 3, 0, -1, 0, -1, 0, 3, 0, -1, 0, -5, 0, 15, 0, -5, 0, -1, 0, 3, 0, -1, 0, -1, 0, 3, 0, -1] \tag{13}$$

The output of matched filter of $B_{3,5}$ is shown in figure 3. Although the main peak level (MPL) increased 5 times relative to the main peak of the child code, the PSL increased by the length of both child code and parent code. Equation (13) shows that the main lobe is 15 which equal to the code length of $B_{3,5}$ and the PSL is 5. The PSLR in this case is -9.54 dB which equal to the PSLR of Barker code B_3 . Table (1) shows that the PSLR is always equivalent to the PSLR of the smallest code length in the nested chain.

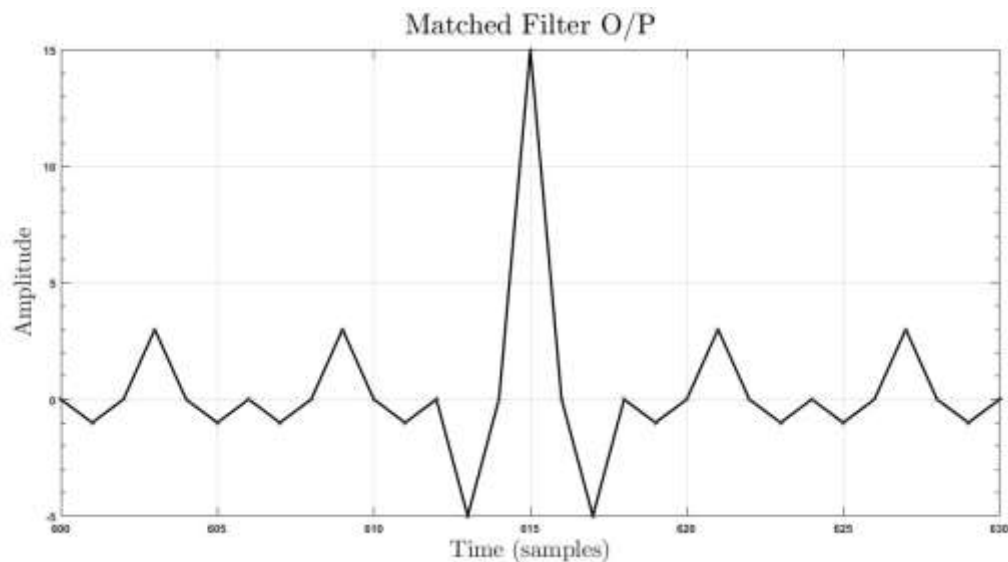


Fig.3. Output of matched filter of code $B_{3,5}$

Table 2: PSLR of some nested compound codes

| Code | MPL | PSL | PSLR (dB) |
|--------------------------|-------|------|-----------|
| B ₃ | 3 | 1 | 9.54 |
| B ₁₃ | 13 | 1 | 22.28 |
| B _{3,3} | 9 | 3 | 9.54 |
| B _{7,3} | 21 | 7 | 9.54 |
| B _{11,7} | 77 | 11 | 16.9 |
| B _{13,3} | 39 | 13 | 9.54 |
| B _{13,13} | 169 | 13 | 22.28 |
| B _{11,7,3} | 231 | 77 | 9.54 |
| B _{13,11,5} | 715 | 143 | 13.98 |
| B _{13,13,13} | 2197 | 169 | 22.28 |
| B _{13,13,13,13} | 28561 | 2197 | 22.28 |

3. Sidelobes cancelation filter for Nested Compound Codes

The sidelobes of the ACF represents a back door for the appearance of false alarms. So, their reduction or cancellation is an objective of old and recent researches. The optimum filter for sidelobes cancellation of nested compound codes should include the cancellation of the child and parent sidelobes.

The ACF of the compound code B_{3,5} in the frequency domain is on the form:

$$\begin{aligned}
 R(e^{j\omega}) = & -1 + 3e^{-2j\omega} - e^{-4j\omega} \\
 & - e^{-6j\omega} + 3e^{-8j\omega} - e^{-10j\omega} \\
 & - 5e^{-12j\omega} + 15e^{-14j\omega} - 5e^{-16j\omega} \\
 & - e^{-18j\omega} + 3e^{-20j\omega} - e^{-22j\omega} \\
 & - e^{-24j\omega} + 3e^{-26j\omega} - e^{-28j\omega}
 \end{aligned} \tag{14}$$

Equation (14) is simplified to:

$$R(e^{j\omega}) = e^{-14j\omega} (3 - 2\cos 2\omega)(5 + 2\cos 6\omega + 2\cos 12\omega) \tag{15}$$

Equation (15) contains two parts, the main lobe, and the sidelobes, namely:

$$R(e^{j\omega}) = M(e^{j\omega}) + S(e^{j\omega}) \tag{16}$$

Where: $M(e^{j\omega})$ represents the main lobe and $S(e^{j\omega})$ represents the sidelobes.

For the compound code B_{3,5}, $M(e^{j\omega})$ is given by:

$$M(e^{j\omega}) = 15e^{-14j\omega} \tag{17}$$

Using the concept of inverse filter, the transfer function of the proposed filter $H_{op}(e^{j\omega})$ is:

$$H_{op}(e^{j\omega}) = M(e^{j\omega}) * [R(e^{j\omega})]^{-1} \tag{18}$$

Where $[R(e^{j\omega})]^{-1}$ is the reciprocal of $[R(e^{j\omega})]$

Substitution for M and R yields:

$$H_{op_{3,5}}(e^{j\omega}) = \frac{15}{(3 - 2\cos 2\omega)(5 + 2\cos 6\omega + 2\cos 12\omega)} \tag{19}$$

The general formula of optimum filter for all Barker code lengths is:

$$H_{op_N}(e^{j\omega}) = \frac{N}{N - 2 \sum_{i=1}^{\frac{N-1}{2}} \alpha_i \cos(2i\omega)} \tag{20}$$

Where α_i is the sidelobes coefficients

The transfer function in (19) for code B_{3,5} consists of two cascaded filters H_{op3} and H_{op5} as following:

$$H_{op_{3,5}}(e^{j\omega}) = H_{op_3}(e^{j\omega})H_{op_5}(e^{j3\omega}) \tag{21}$$

Figure 4 shows the output from optimum filter of the nested compound code B_{3,5}:

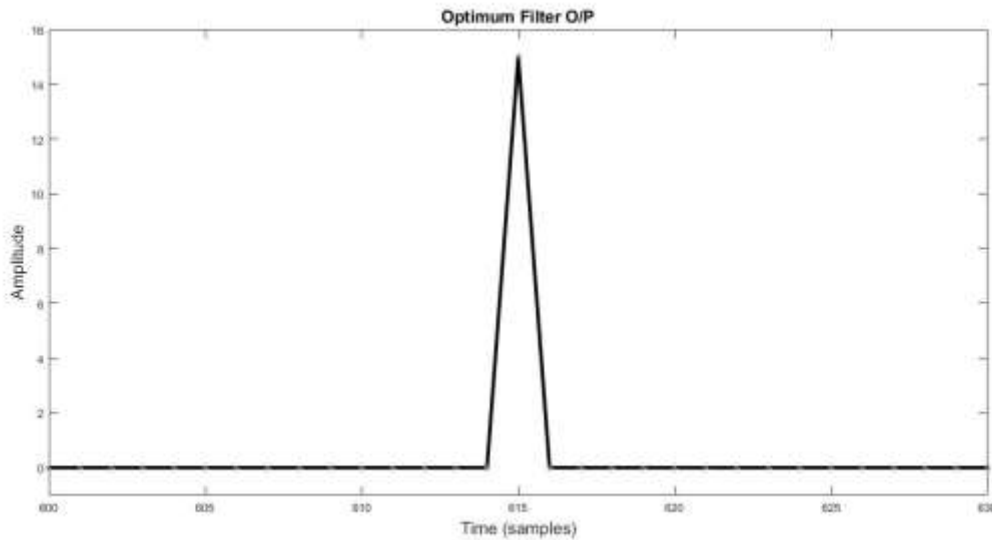


Fig.4. Optimum filter results from Nested Compound Code B_{3,5}

By conduction of equation (21) for any compound code (B_{N₁,N₂}) is:

$$H_{opN_1,N_2}(e^{j\omega}) = H_{opN_1}(e^{j\omega})H_{opN_2}(e^{jN_1\omega}) \quad (22)$$

The generalization of equation (22) for any nested compound code could be obtained following the same approach to get a general form for transfer function of the optimum filter for L level nested compound code (B_{N₁,N₂...N_L}):

$$H_{opN_1,N_2\dots N_L}(e^{j\omega}) = H_{N_1}(e^{j\omega}) \prod_{i=2}^L H_{N_i}(e^{j\prod_{k=1}^{i-1} N_k\omega}) \quad (23)$$

The processor of binary phase coded signal with free sidelobes is composed of two parts, the matched filter and the optimum filter as shown in figure 5.

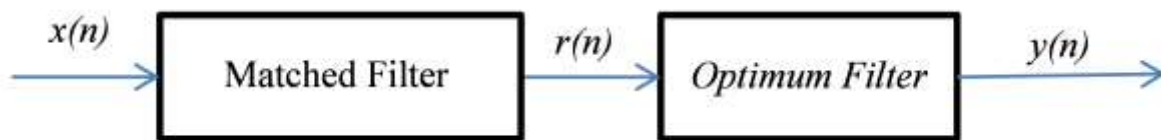


Fig.5. Sidelobes cancellation processor using proposed optimum filter

4. Realization of nested compound code processor

From equation (11), the encoder is simply realized as cascading L filters with the same barker coder hardware structure and changing the filter delay in each stage depending on the code length in previous stages as shown in figures 6.

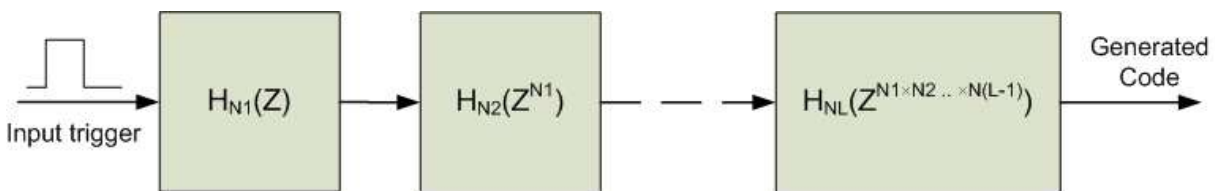


Fig.6. Encoder of Nested Compound Codes

From equation (12), the matched filter also can be realized as cascaded filters as shown in figure 7.

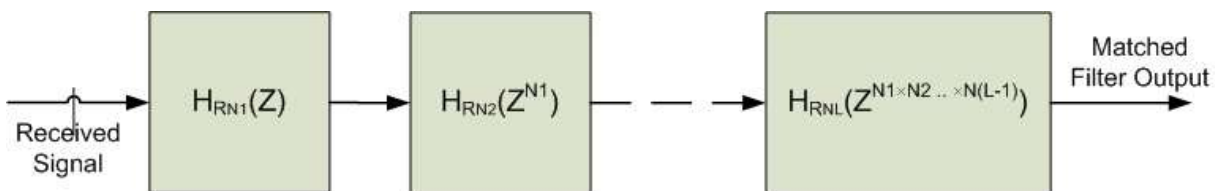


Fig.7. Matched Filter of Nested Compound Codes

Figure 8 shows that to generate code B_{3,5}, the encoder of Barker codes B₃ and B₅ are used consecutively with the same hardware structure and only changing is the delay line length in B₅ encoder to be three samples.

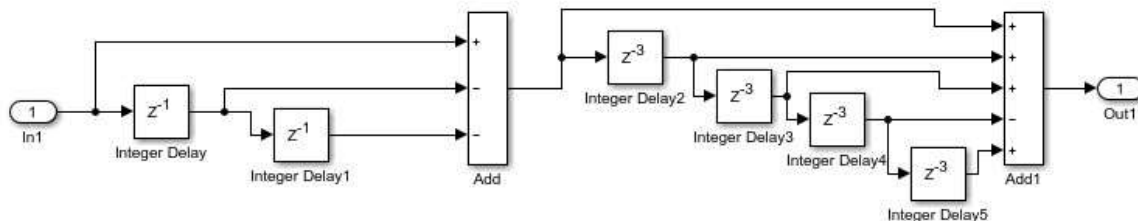


Fig.8. Encoder of Nested Compound Codes B_{3,5}

The decoder is realized with the same manner as shown in figure 9.

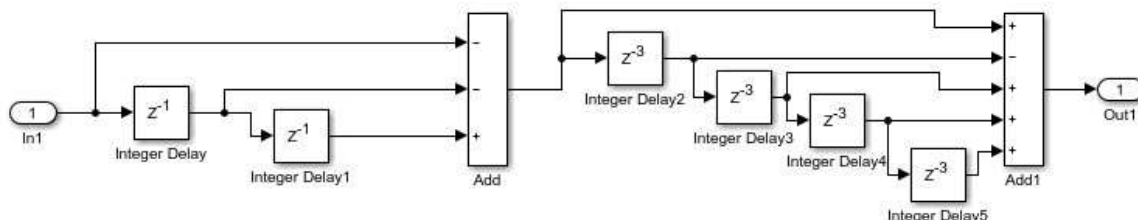


Fig.9. Decoder of Nested Compound Codes B_{3,5}

Equation 23 shows that the optimum filter for L levels nested compound code is also realized as cascaded filters in frequency domain as shown in figure 10. The output from the matched filter $r(n)$ is applied to Fast Fourier Transformation (FFT) with length (equal to) or (more than) the whole range cells (zeros could be added in front or back of $r(n)$ to make the length equal 2^k). The coefficients of the optimum filter $H_{opN}(e^{j\omega})$ are offline calculated in ω domain $[-\pi, \pi[$ for each level, sampled with the same FFT length and stored in memory. These coefficients are sequentially multiplied to the output of FFT to get the output in frequency domain $Y(e^{j\omega})$. To retrieve the output in time domain, Inverse Fast Fourier Transformation (IFFT) is used.

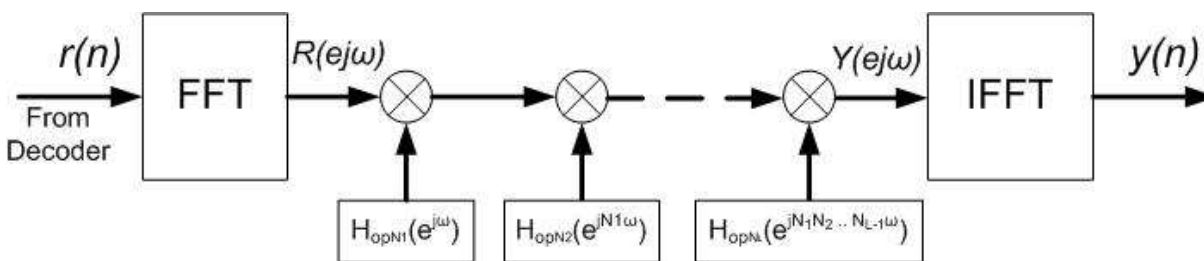


Fig.10. Optimum filter of Nested Compound Codes

5. Performance Analysis of The Nested Compound Optimum Filter

To investigate the performance of proposed optimum filter for nested compound codes, the Radar chain shown in figure (11) is used. The MTI in the following scenarios is disabled to put the sidelobe cancellation processor in severe conditions to study its effect in detecting both moving and stationary targets and also to prevent the MTI from affecting or reducing the clutter. The processing passes through coherent processing interval (CPI). The CPIs divided into 32 transmitted pulse (T_r). The whole CPI is coherently integrated in the 'Azimuth FFT' filter to find the Doppler cells. Each cell passes to the CFAR processor for detection. CFAR processor is used for target detection with probability of false alarm ($P_{fa}=10^{-6}$). The CFAR uses 'Smallest of (SOF)' algorithm. This algorithm is designed to has good detection for neighboring targets. On the other hand, this tends to increase the probability of false alarm specially, in the presence of inhomogeneous clutter or high sidelobes [7]. To illustrate the enhancement in target detection, some scenarios have been assumed in the following section.

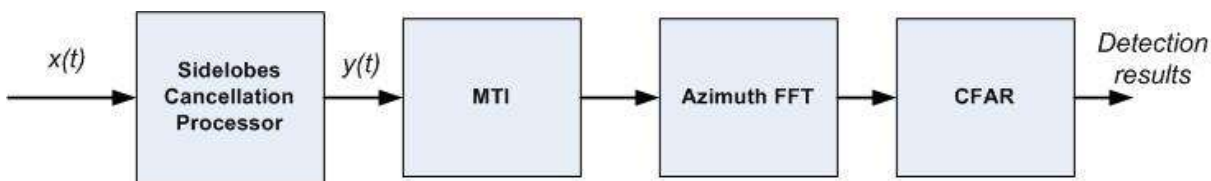


Fig.11. Radar Chain contains the proposed sidelobes cancellation filter

5.1 Noise free case

5.1.1 Detection of Stationary Targets

In this scenario, we assumed that there is a stationary target. The sidelobes cancellation processor shown in figure (5) is only used in this scenario to find the improvement in performance using the nested code optimum filter. The input code is $B_{13,13}$. Figure (12) shows a very high undesired sidelobes in case of using matched filter alone. While, figure (13) shows that all these sidelobes are totally eliminated without any loses in the main lobe peak.

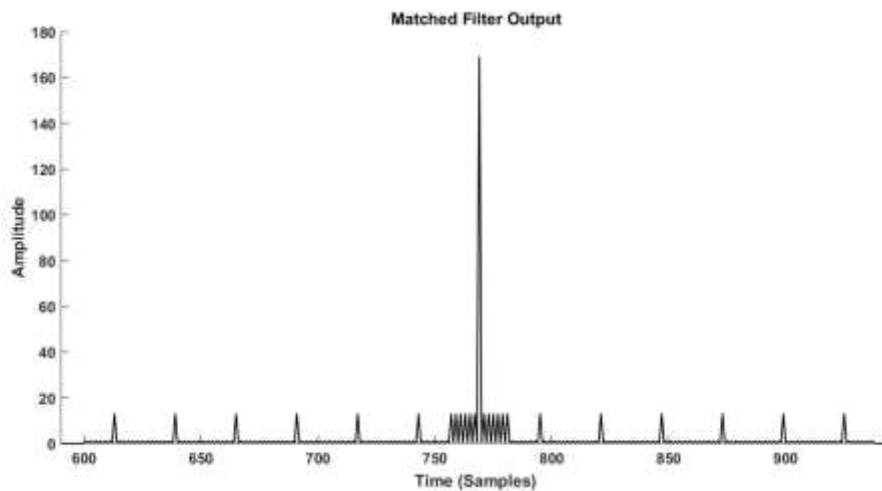


Fig.12. Matched filter output using nested code $B_{13,13}$

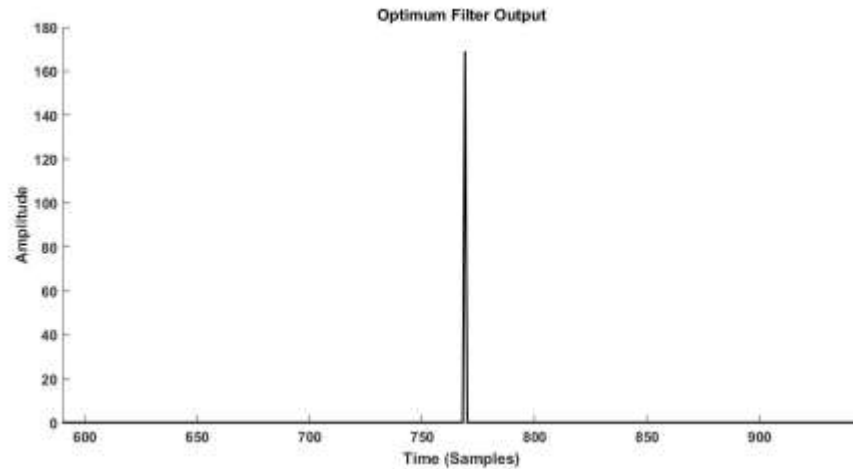


Fig.13. Optimum filter output using nested code B_{13,13}

5.1.2 Detection of moving target

In the case of moving targets, the target motion causes phase shift equal to $\phi_n = 2\pi f_d t$. This phase shift appears in the received signal as shown in equation (24):

$$s(nT_s) = x(nT_s) \cos(2\pi f_d(nT_s)) \tag{24}$$

where f_d is the Doppler frequency and T_s is the pulse sampling period.

The Doppler effect varies the matched filter output. This variation affects both main lobe and sidelobes and leads to make sidelobes asymmetric around the main lobe as shown in figure (14). This asymmetry causes the appearance of residue sidelobes remaining in the output of optimum filter as shown in figure (15).

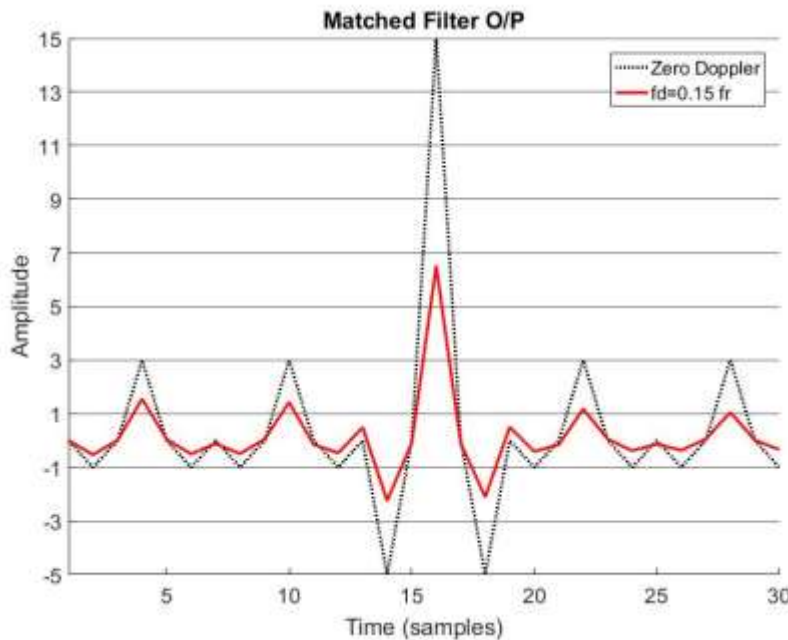


Fig.14. Matched filter output of code B_{3,5} for moving target at certain period

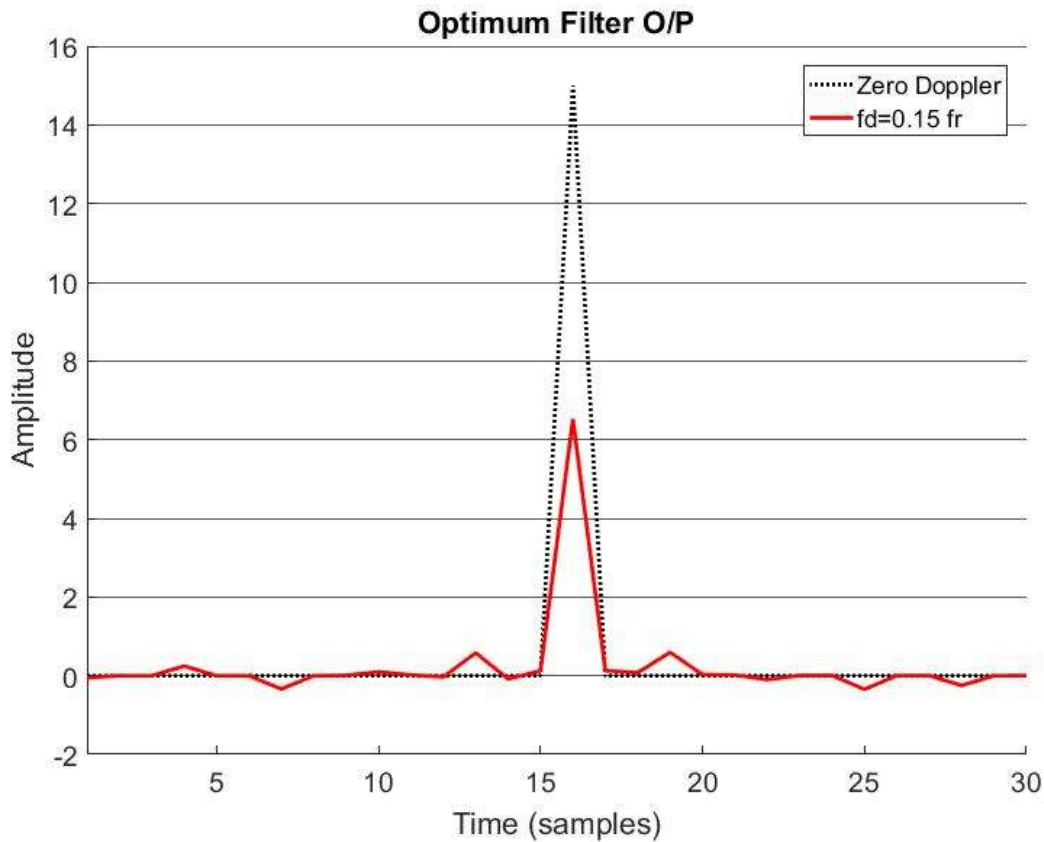


Fig.15. Optimum filter output of code B_{3,5} for moving target at certain period

In pulse-Doppler radar, the detection is performed over multiple T_r . These multiple T_r periods are recorded and processed in azimuth FFT to calculate the Doppler frequency over all range cells. For real signal, the maximum unambiguous Doppler is $f_{d(max)} = 0.5f_r$. Assuming a fixed sampling frequency f_s , Changing the code length or total samples affects the pulse duty cycle. Also, changing the total samples affects the pulse repetition frequency (PRF) f_r . We shall demonstrate two different cases depending on the PRF and the pulse duty cycle.

A. High PRF case (duty cycle above 10%):

Using high PRF leads to no Doppler ambiguity on the targets in a large range of target velocities but this causes range ambiguity. In pulse compression phase coded signal, increasing the Doppler frequency decreases PSLR for matched filter and consequently for optimum filter. For example, assume the total range cells are 1024 and the code length is 169, the duty cycle becomes approximately 16.5%. Figure (16) shows that the optimum filter performance is degraded versus increasing the Doppler frequency. For both matched and optimum filter, the whole performance decreased when $f_d > 0.42f_r$.

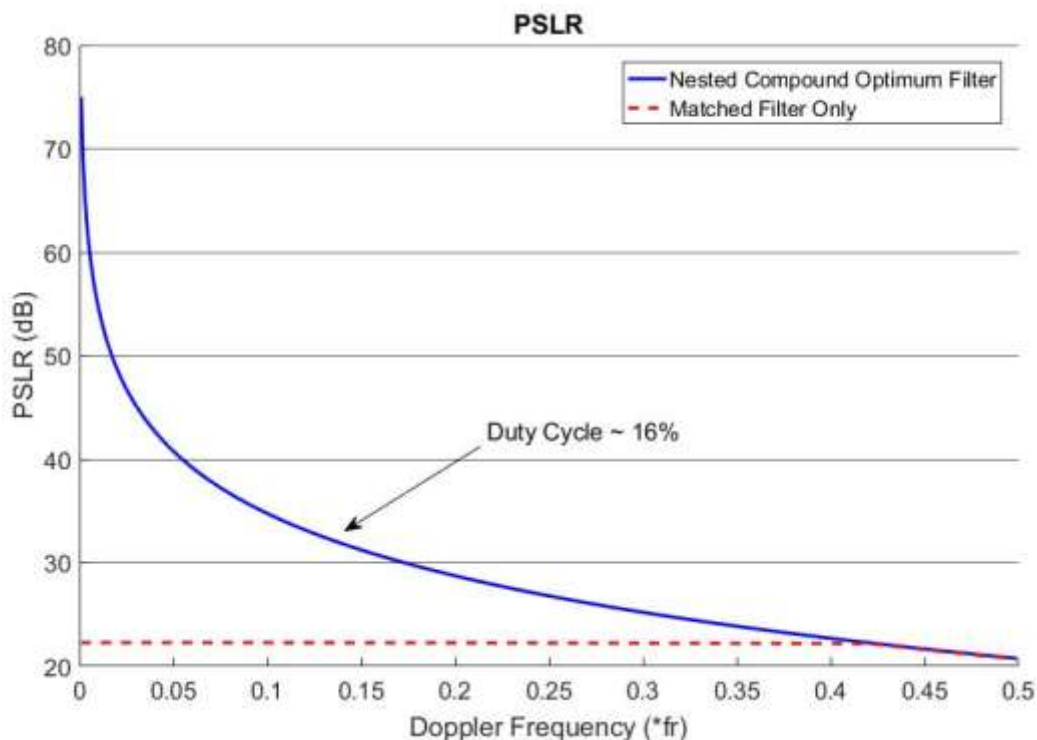


Fig.16. PSLR measures of code (B_{13,13}) versus Doppler phase shift (Assuming Total samples=1024)

B. Low PRF case (duty cycle below 10%):

Using low duty cycle decreases the range ambiguity for targets but this limits $f_{d(max)}$. Figure (17) shows that the performance of using matched filter only is approximately the same for the whole f_d range. The optimum filter performance decreases versus increasing f_d and increases by decreasing the duty cycle.

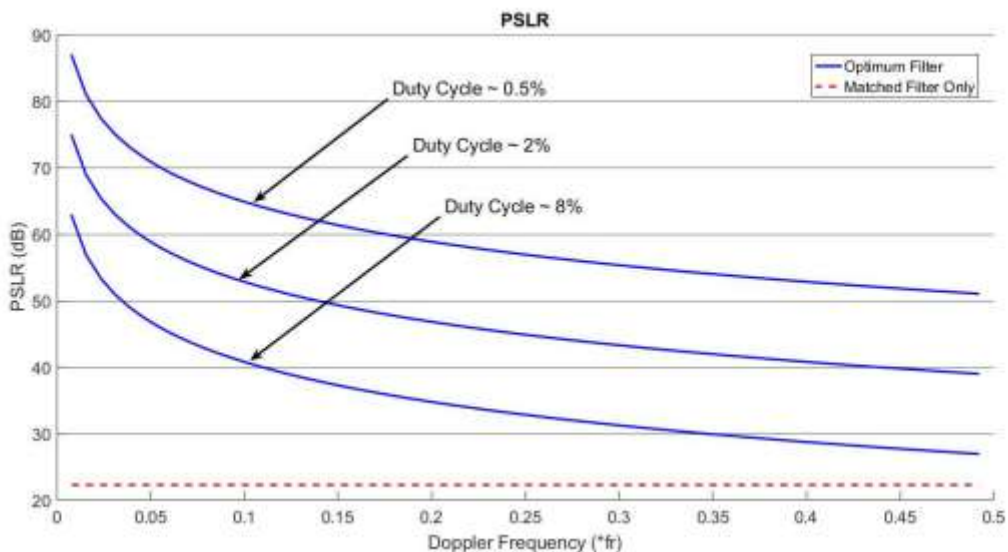


Fig.17. Enhancement in optimum filter performance by decreasing the duty cycle

For all above cases, the performance of the proposed sidelobe cancellation processor using the optimum filter is still better than using the matched filter alone for all Doppler frequency and the optimization between these parameters depends on the application.

5.2 Normal Gaussian Noise case

5.2.1 Static Target Detection

To detect static targets, both MTI and azimuth FFT are functionally disabled in this scenario to focus on the improvement from optimum filter compared to matched filter only. By adding normal Gaussian noise with signal to noise ratio ($S/N = 10\text{dB}$) to nested code $B_{13,13}$, the output from the matched filter is found to have a high sidelobes level as well as the CFAR processor threshold level is high. The high sidelobes level is detected as false targets in the CFAR processor as shown in figure (18).

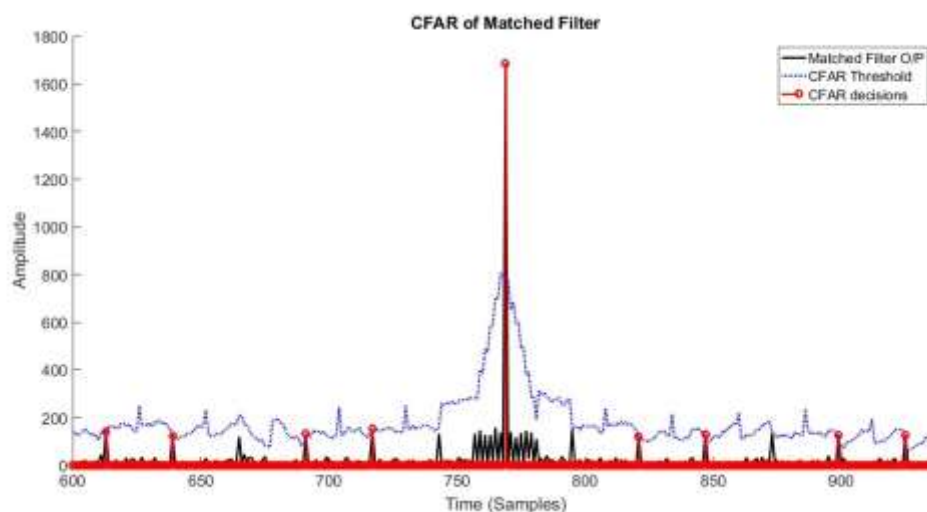


Fig.18. CFAR detection after the matched filter ($S/N = 10\text{dB} - P_{fa} = 10^{-06}$)

Passing this output to the proposed optimum filter, it removes the high sidelobes as shown in figure (19).

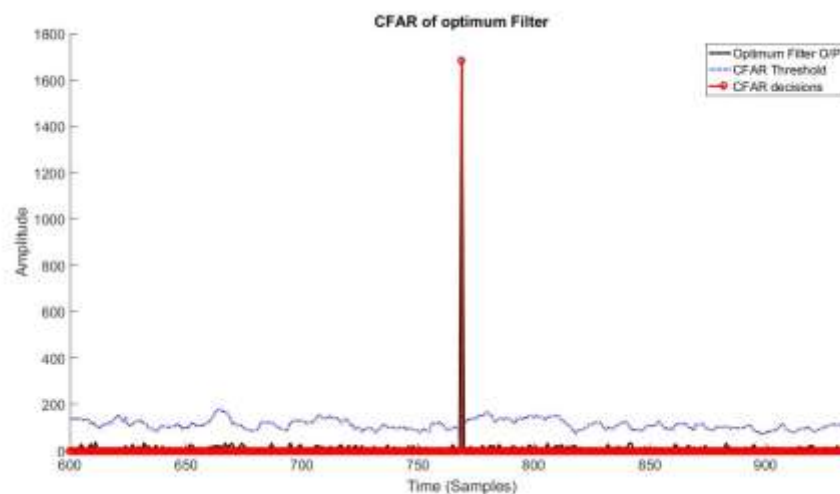


Fig.19. CFAR detection after the optimum filter ($S/N = 10\text{dB} - P_{fa} = 10^{-06}$)

Increasing S/N in the input of the matched filter reduces the sidelobes level until it reaches its limited value which is (22.28 dB) since the sidelobes level increase with the mainlobe level with the same ratio. In our proposed optimum filter, the S/N at the output of the optimum filter almost increases linearly with the increasing in S/N in the input due to the absent of all sidelobes. Also, increasing the code length increases the output S/N as shown in figure (20).

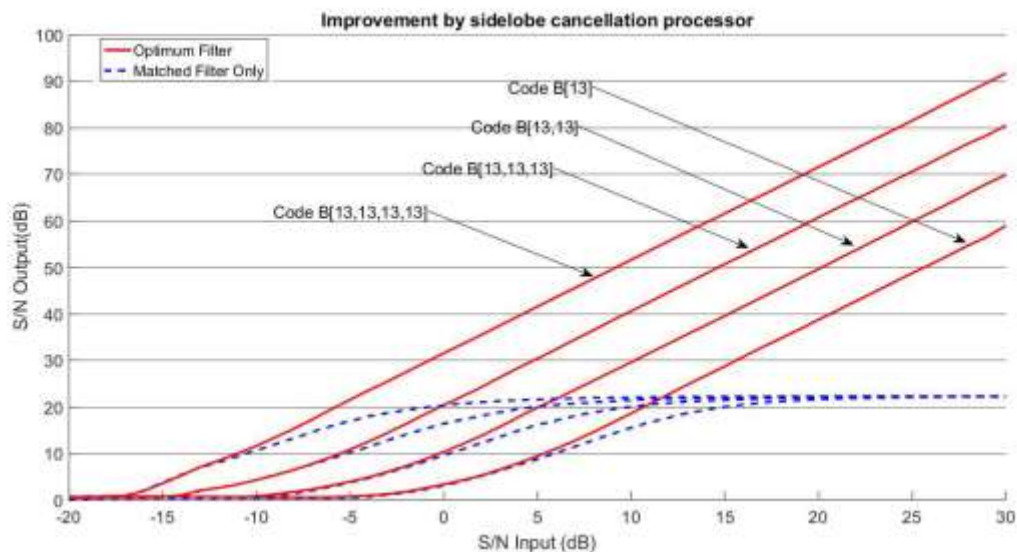


Fig.20. Effect of increasing the target (S/N) on the O/P (S/N) from matched filter and optimum filter

As a result of removing the sidelobes the probability of detection has increased. Figure (21) shows the enhancement in probability of detection obtained by increasing the code length.

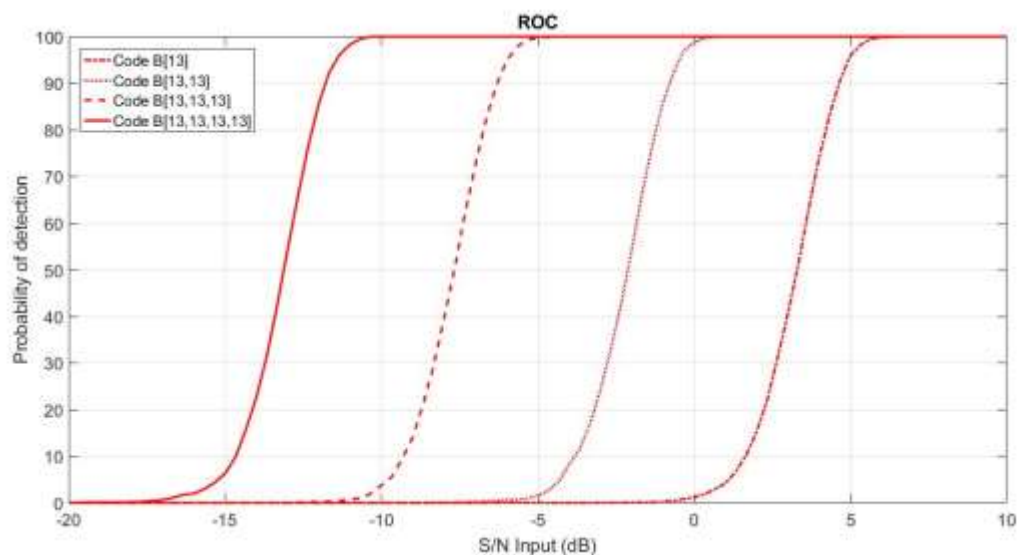


Fig.21. ROC Curve for different codes ($P_{fa}=10^{-6}$)

5.2.2 Moving Target Detection

In the following scenario, the performance of the nested compound optimum filter in case of presence of moving target is presented. The target has (S/N = 10dB) and Doppler frequency ($f_d=0.29f_r$). The

whole receiver processor shown in figure (11) is active excluding the MTI and uses sampling frequency $f_s=2048f_r$. The encoder code is $B_{13,13}$. Figure (22) shows the presence of sidelobes. The nested compound optimum filter removes these sidelobes except some remains due to Doppler effect as shown in figure (23).

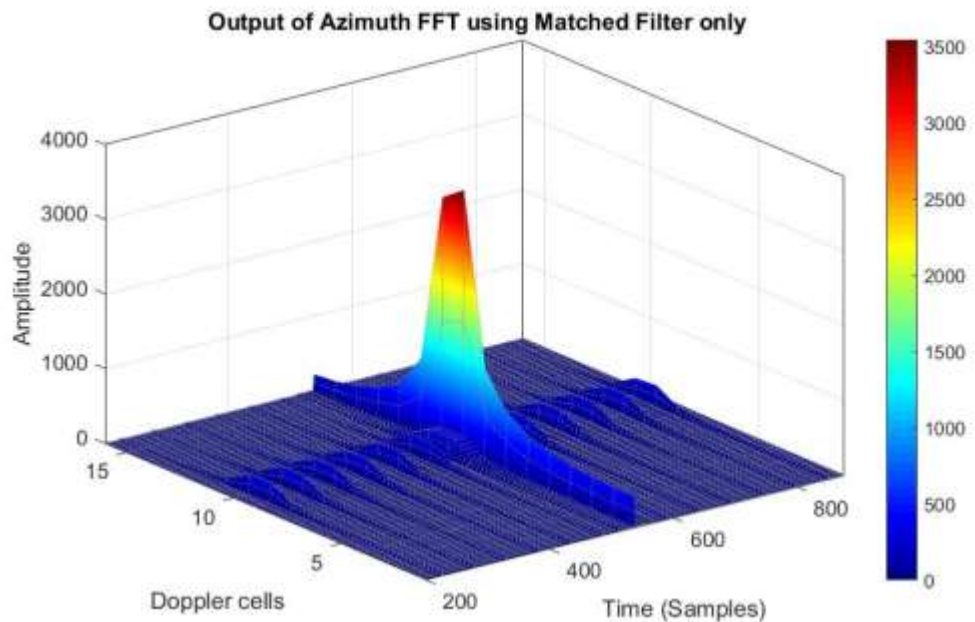


Fig.22. Range-Doppler Map from Azimuth FFT in the case of using matched filter only (Target $f_d=(9.5/32)f_r$)

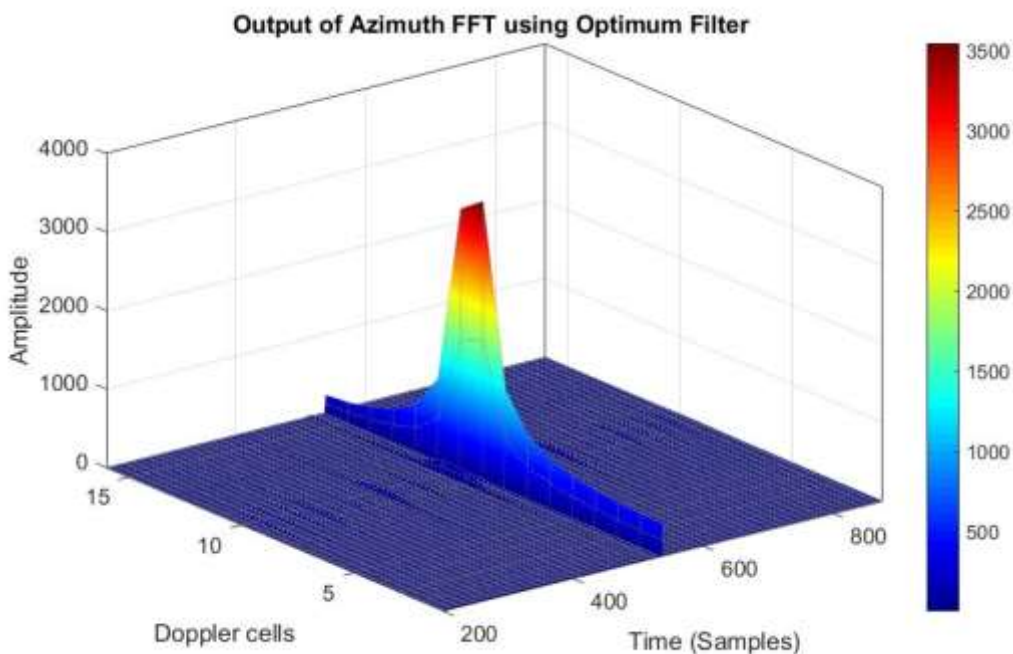


Fig.22. Range-Doppler Map from Azimuth FFT in the case of using Optimum Filter (Target $f_d=(9.5/32)f_r$)

6. Conclusion

In the present work, a novel method for encoding, decoding and sidelobe cancellation at the output of matched filter for long binary nested Barker codes is introduced. The detection performance (P_d) of the proposed nested compound optimum filter has increased over the matched filter in the presence of normal Gaussian noise. The sensitivity to the Doppler effect is found to be less than that of the Matched filter alone.

References

- [1] Skolnik, M. I., "Introduction to Radar Systems (3rd ed.)." New York: McGraw-Hill, 2001, 339—369
- [2] Barker, R. H., "Group synchronization of binary digital systems," In W. Jackson (Ed.), Communication Theory, Burlington, MA: Academic Press, 1953.
- [3] A. N. Leukhin, E. N. Potekhin, Optimal peak sidelobe level sequences up to length 74, in: Radar Conference (EuRAD), 2013 European, IEEE, 2013, pp. 495–498.
- [4] C. J. Nunn, G. E. Coxson, Best-known autocorrelation peak sidelobe levels for binary codes of length 71 to 105, IEEE transactions on Aerospace and Electronic Systems 44 (1).
- [5] E. E. Hollis, Predicting the truncated autocorrelation functions of combined barker sequences of any length without use of a computer, IEEE Transactions on Aerospace and Electronic Systems AES-3 (2) (1967) 368–369. doi:10.1109/TAES.1967.5408763.
- [6] A. H. Elbardawiny, A. Sobhy, A novel sidelobe cancellation method for barker code pulse compression, AEROSPACE SCIENCES AND AVIATION TECHNOLOGY, ASAT 17.
- [7] A. Moustafa, F. M. Ahmed, K. Moustafa, Y. Halwagy, A new cfar processor based on guard cells information, in: Radar Conference (RADAR), 2012 IEEE, IEEE, 2012, pp. 0133–0137.